

Electron Transfer Reactions of Fluorotyrosyl Radicals

Steven Y. Reece, Mohammad R. Seyedsayamdost, JoAnne Stubbe, and Daniel G. Nocera*

Department of Chemistry, Massachusetts Institute of Technology, 77 Massachusetts Avenue,
Cambridge, Massachusetts 02139-4307

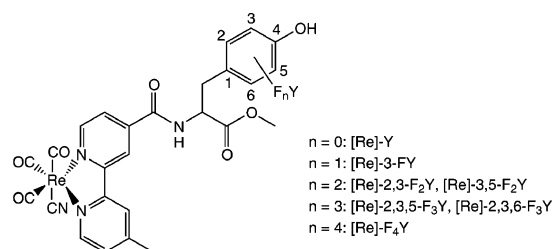
Received May 25, 2006; E-mail: nocera@mit.edu

Amino acid radicals have emerged as prominent redox-active cofactors and charge transfer intermediates in enzymes. The tyrosyl radical, Y^{\bullet} , is particularly prevalent and is found in many systems, including photosystem II (PS II),¹ prostaglandin synthase,² galactose oxidase,³ and ribonucleotide reductase (RNR).⁴ Nature employs tyrosine to fulfill two enzymatic criteria: (1) as a charge transport relay and (2) to transport both a proton and an electron for the activation of substrates at an enzyme active site. In either case, proton-coupled electron transfer, PCET, is implicated as the mechanism for charge transport by Y^{\bullet} owing to its high oxidation potential when protonated.⁵ Our studies have highlighted the PCET among the many tyrosines composing the radical hopping pathway in class I RNR.^{4,6} One approach to studying radical transport in RNR is to photochemically generate Y^{\bullet} with an excited state oxidant and kinetically monitor its reactivity with transient spectroscopy. The excited states of Re^I complexes are competent for Y oxidation, either directly⁷ or via the “flash-quench” technique.⁸ Furthermore, fluorotyrosines, F_nY , are powerful tools for disentangling the role of the proton and electron in RNR⁹ since the F_nY redox potential depends on the pK_a and pH-independent reduction potential.¹⁰ From the perspective of PCET kinetics investigation, these non-natural amino acids are useful, as well, since the absorption spectrum of the tyrosine radical varies with fluorination. However, the kinetics for photogeneration of F_nY^{\bullet} and its lifetime have yet to be defined. Knowledge of both is needed for the implementation of these radicals in untangling biological PCET mechanisms. We now show that the excited state of a Re^I polypyridyl complex can directly photooxidize F_nY^- (Chart 1), and that the kinetics for charge separation are in the normal Marcus regime, whereas charge recombination is inverted.

The complex, $Re(bpy)(CO)_3CN$ ($= [Re]$), is a powerful excited state oxidant ($E^{\circ}(Re^{I*}/0) = 1.6$ V vs NHE). When the native amino acid, Y , is appended to the bpy ligand in $[Re]-Y$ ($n = 0$, Chart 1), excited state quenching ensues and Y^{\bullet} forms when the tyrosine phenol is deprotonated.⁷ We now have prepared the series of $[Re]-F_nY$ presented in Chart 1 to determine how variation in the F_nY^-/F_nY^{\bullet} reduction potential affects the rate of radical formation and charge recombination. The details of synthesis and characterization are presented in the Supporting Information. Briefly, the compounds were obtained by coupling the previously reported series of fluorotyrosine methyl esters with $Re(bpy-COOH)(CO)_3CN$ using standard amide bond peptide coupling chemistry in modest yield (25–50%). In the course of this work, single crystals of $Re(bpy-COOH)(CO)_3CN$ were obtained. The solution of the X-ray crystal structure is presented in the Supporting Information as this is the first reported structure of a mononuclear $Re(bpy)(CO)_3CN$ complex. Of note, the weaker field CN^- ligand results in a longer $Re-C$ bond length of 2.17 Å compared to the shorter $Re-C$ bond lengths of the stronger field, facial CO ligands (1.92–1.95 Å).

Ultrafast time-resolved emission and nanosecond transient absorption spectroscopies were undertaken on $[Re]-F_nY^-$ complexes to characterize kinetically any photoinduced electron transfer. All

Chart 1. Structure of $[Re]-F_nY$ Complexes



spectroscopy was performed on compounds dissolved in aqueous solutions of 10 mM KOH (pH 12) in the concentration range of 50–100 μ M and freeze–pump–thaw degassed to 10^{-5} Torr. Laser radiation (400 nm, ~ 100 fs) was used as the pump source in the time-resolved emission experiments, and the data were collected on a streak camera as previously described.⁷ For each $[Re]-F_nY^-$, the excited state $[Re]$ emission was quenched compared to $[Re]-Y$ at pH 7 and could be fit to a single exponential decay function. The emission quenching is due to electron transfer⁷ to the excited Re complex from F_nY^- and the rate of charge separation, k_{CS} , could be determined from

$$k_{CS} = \tau^{-1}([Re]-F_nY^-) - \tau^{-1}([Re]-Y) \quad (1)$$

where $\tau([Re]-F_nY^-)$ is the emission lifetime of the quenched complex at pH 12 and $\tau([Re]-Y)$ is the lifetime of the unquenched control at pH 7. These data are presented in tabular form in the Supporting Information, and k_{CS} varies from 89.2 to 2.15×10^7 s^{-1} depending on the F_nY employed.

Nanosecond transient absorption spectroscopy confirms that the emission quenching is due to electron transfer in the $[Re]-F_nY^-$. Figure 1 shows the transient spectra observed following 355 nm (fwhm = 3 ns) excitation of $[Re]-2,3,6-F_3Y^-$. The peak at 520 nm corresponds to the reduced $bpy^{\bullet-}$ ligand,⁷ and the peak at 418 nm corresponds to the absorption feature for $2,3,6-F_3Y^{\bullet}$.⁹ The spectra at 15 and 65 ns are somewhat different, however, as the ratio of the 520/480 nm peaks changes slightly. These dynamics are due to the decay of the quenched 3MLCT state which occurs with a time constant of 14.5 ns obtained from the ultrafast emission quenching described above. As such, the single wavelength kinetics trace obtained at 520 nm in the inset of Figure 1 (and for the other F_nY^- with $n \geq 2$) was fit starting at 20 ns with a sum of two exponentials: a fast growth component whose time constant was fixed to that obtained in the ultrafast emission experiment and a slow decay component. The latter component corresponds to charge recombination (CR), the rate constants for which, k_{CR} , are presented in tabular form in the Supporting Information. For F_nY^- with $n < 2$, the quenched 3MLCT state decayed within the instrument response, and thus the 520 nm traces could be fit to a single exponential.

With the rates for charge separation and recombination in $[Re]-F_nY^-$ in hand, we next chose to analyze the driving force

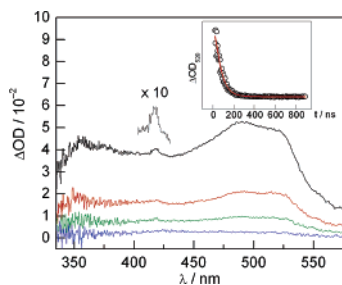


Figure 1. Transient absorption spectra of [Re]-2,3,6-F₃Y⁻ observed (black line) 15, (red line) 65, (green line) 115, and (blue line) 215 ns and following 355 nm, 3 ns laser irradiation. The Y⁻ absorbance feature of the 15 ns trace is magnified. Inset: Single wavelength kinetics trace (○) obtained at 520 nm with biexponential fit (red line).

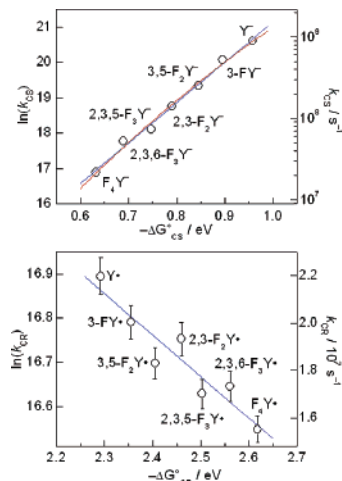


Figure 2. Top: $\ln(k_{CS})$ versus $-\Delta G_{CS}^{\circ}$ plot with linear (blue line) and parabolic (red line) fit. Bottom: $\ln(k_{CR})$ versus $-\Delta G_{CR}^{\circ}$ plot with linear (blue line) fit.

dependence of these rates within the Marcus–Levich framework for ET described by eq 2:¹¹

$$k_{ET} = \sqrt{\frac{\pi}{\hbar^2 \lambda k_B T}} |V|^2 \exp\left[-\frac{(\Delta G^{\circ} + \lambda)^2}{4\lambda k_B T}\right] \quad (2)$$

where V is the electronic coupling, λ is the reorganization energy, and ΔG° is the free energy driving force for the electron transfer. The driving force for the CS and CR reactions, ΔG_{CS}° and ΔG_{CR}° , were derived from eqs 3 and 4, respectively

$$-\Delta G_{CS}^{\circ} = E^{\circ}(\text{Re}^{I^{*0}}) - E_p(\text{F}_n\text{Y}^{\bullet}/\text{F}_n\text{Y}^{-}) \quad (3)$$

$$\Delta G_{CR}^{\circ} = E^{\circ}(\text{Re}^{I/0}) - E_p(\text{F}_n\text{Y}^{\bullet}/\text{F}_n\text{Y}^{-}) \quad (4)$$

where $E^{\circ}(\text{Re}^{I^{*0}})$ and $E^{\circ}(\text{Re}^{I/0})$ are the excited and ground state Re^I reduction potentials⁷ and $E_p(\text{F}_n\text{Y}^{\bullet}/\text{F}_n\text{Y}^{-})$ is the peak potential for the F_nY[•]/F_nY⁻ couple.⁹ Figure 2 (top) plots $\ln(k_{CS})$ versus $-\Delta G_{CS}^{\circ}$ and shows that the data are well fit by both a linear and parabolic Marcus relation. These data indicate that CS is strongly activated and occurs in the normal region for Marcus' ET. In the limit that $4\lambda \gg \Delta G^{\circ 2}$, eq 2 predicts that the $\ln(k_{CS})$ versus $-\Delta G_{CS}^{\circ}$ plot should be linear with a slope of $0.5/(k_B T)$. From the linear fit in Figure 2 (top), we obtain $0.3/(k_B T)$. The parabolic fit (eq 2) yields an approximate value of λ for this system of 1.9 eV, indicating that 4λ is about an order of magnitude larger than $\Delta G^{\circ 2}$. The temperature dependences of k_{CS} for [Re]-3,5-F₂Y and [Re]-F₄Y are consistent with this value of λ (see Supporting Information for details).

Figure 2 (bottom) plots $\ln(k_{CR})$ versus $-\Delta G_{CR}^{\circ}$ and, in contrast to CS, shows that CR is weakly dependent on driving force and occurs in the inverted region for Marcus' ET. Previous work has shown that inverted region ET often does not exhibit the predicted parabolic dependence on driving force due to electron coupling to vibrational modes that assist the reaction.¹² Under such conditions, a modest linear decrease in $\ln(k_{CR})$ with $-\Delta G_{CR}^{\circ}$ is predicted by the energy gap law.¹² The scatter in these data is likely due to experimental precision (2 ns error shown in plot) and small differences in electronic coupling and/or frequency of the accepting vibrational modes for each of the F_nYs.

With the basic model of electron transfer in the [Re]-F_nY in hand, future work will focus on incorporation of this system into RNR for the study of photoinitiated radical transport. Radical transport in the enzyme likely occurs via a PCET mechanism as amino acid oxidation is coupled to changes in protonation state. Upon substituting F_nY for Y, we can now predict what affect this will have on the ET part of the reaction, allowing us to gauge the degree of proton coupling to the radical transport process.

The ability to phototrigger radical formation is a powerful tool for the study of radical-based enzymes. Previous methods to generate the radicals by metal complexes have relied on indirect bimolecular methods (flash-quench¹³) owing to insufficient oxidizing power of the direct excited state. As we show here, this is not the case for Re^I polypyridyl excited states. Transient spectroscopic results show that a tyrosyl radical is generated promptly upon photoexcitation, and it is of sufficient lifetime to promote the investigation of radical transport. One important reason for the prompt photogeneration is that the non-natural F_nY amino acids are deprotonated at physiological pHs so that radical initiation occurs by simple electron transfer. Using previously described peptide methods,¹⁰ the [Re]-F_nY constructs may be incorporated into the PCET network of RNR, thus allowing the kinetics for radical transport to be probed. These studies are now underway.

Acknowledgment. We thank Justin M. Hodgkiss and Elizabeth R. Young for assistance with ultrafast spectroscopy, Arthur Esswein for help with X-ray crystallography, and the National Institutes of Health for support of this work GM47274 (D.G.N.) and GM29595 (J.S.).

Supporting Information Available: Synthetic details and characterization data for the [Re]-F_nY series, X-ray crystallographic data for Re(bpy-COOH)(CO)₃CN, emission quenching and charge recombination kinetics data for [Re]-F_nY complexes in tabular form, and data and analysis for temperature dependence of k_{CS} for [Re]-3,5-F₂Y and [Re]-F₄Y. This material is available free of charge via the Internet at <http://pubs.acs.org>.

References

- (1) Tommos, C.; Babcock, G. T. *Biochim. Biophys. Acta* **2000**, *1458*, 199.
- (2) Tsai, A.-L.; Palmer, G.; Xiao, G.; Swinney, D. C.; Kulmacz, R. J. *J. Biol. Chem.* **1998**, *273*, 3888.
- (3) Whittaker, J. W. *Chem. Rev.* **2003**, *103*, 2347.
- (4) Stubbe, J.; Nocera, D. G.; Yee, C. S.; Chang, M. C. Y. *Chem. Rev.* **2003**, *103*, 2167.
- (5) Mayer, J. M. *Annu. Rev. Phys. Chem.* **2004**, *55*, 363.
- (6) Reece, S. Y.; Hodgkiss, J. M.; Stubbe, J.; Nocera, D. G. *Philos. Trans. R. Soc. B* **2006**, *361*, 1351.
- (7) Reece, S. Y.; Nocera, D. G. *J. Am. Chem. Soc.* **2005**, *127*, 9448.
- (8) Miller, J. E.; Di Bilio, A. J.; Wehbi, W. A.; Green, M. T.; Museth, A. K.; Richards, J. R.; Winkler, J. R.; Gray, H. B. *Biochim. Biophys. Acta* **2004**, *1655*, 59.
- (9) Seyedsayamdost, M. R.; Reece, S. Y.; Nocera, D. G.; Stubbe, J. *J. Am. Chem. Soc.* **2006**, *128*, 1569.
- (10) Seyedsayamdost, M. R.; Yee, C. S.; Reece, S. Y.; Nocera, D. G.; Stubbe, J. *J. Am. Chem. Soc.* **2006**, *128*, 1562.
- (11) Marcus, R. A.; Sutin, N. *Biochim. Biophys. Acta* **1985**, *811*, 265.
- (12) Chen, P.; Meyer, T. J. *Chem. Rev.* **1998**, *98*, 1439.
- (13) Sjödin, M.; Styring, S.; Wolpher, H.; Xu, Y.; Sun, L.; Hammarström, L. *J. Am. Chem. Soc.* **2005**, *127*, 3855.

JA0636688